Journal of Molecular Spectroscopy 286–287 (2013) 12–20

Contents lists available at SciVerse ScienceDirect

Journal of Molecular Spectroscopy

journal homepage: www.elsevier.com/locate/jms

A general analytical expression for the three-dimensional Franck–Condon integral and simulation of the photodetachment spectrum of the PO_2^- anion

Jun Liang [a,*], Fang Cui [a], Ru Wang [a], Wei Huang [b,*,1], Zhifeng Cui [a]

[a] Institute of Atomic and Molecular Physics, College of Physics and Electronic Information, Anhui Normal University, Wuhu 241000, PR China
[b] Laboratory of Atmospheric Physico-Chemistry, Anhui Institute of Optics & Fine Mechanics, Chinese Academy of Sciences, Hefei, Anhui 230031, PR China

ARTICLE INFO

Article history:
Received 9 November 2012
In revised form 23 February 2013
Available online 7 March 2013

Keywords:
Franck–Condon overlap integrals
Photoelectron spectroscopy
Spectral simulation
Hot bands

ABSTRACT

Calculations of Franck–Condon factors are crucial for interpreting vibronic spectra of molecules and studying nonradiative processes. We have derived straightforwardly a more general analytical expression for the calculation of the three-dimensional Franck–Condon overlap integrals on the basis of harmonic oscillator approximation under the influence of mode mixing effects. This new analytical expression was applied to study the photoelectron spectra of PO_2^-. The theoretical spectrum obtained by employing CCSD(T) values is in excellent agreement with the observed one. An 'irregular spacing' observed in the experimental photoelectron spectrum of PO_2^- is interpreted as contributing from a hot-band sequence of the bending vibration ω_2 and combination bands of the stretching vibration ω_1 and the bending vibration ω_2. In addition, the equilibrium geometry parameters, r(O–P) = 1.495 ± 0.005 Å and ∠(O–P–O) = 119.5 ± 0.5°, of the $\tilde{X}^1A_1$ state of PO_2^-, are derived by employing an iterative Franck–Condon analysis procedure in the spectral simulation.

1. Introduction

The distribution of relative intensities among the vibronic bands in the electronic spectra of molecules is governed by the Franck–Condon (FC) principle in the absence of vibronic coupling. Along with the development of experimental high-resolution vibronic spectroscopic techniques, the problem of analyzing the observed spectra is receiving increased attention [1,2]. Assuming that molecules retain their symmetry during the electronic transition, the normal coordinates of electronic states generally undergo a distortion as well as a rotation. The rotation results in a mixing of the normal coordinates and thereby the nonseparability of the multidimensional Franck–Condon integrals. This mode mixing, the Duschinsky effect [3], makes the calculation of multidimensional Franck–Condon integrals a troublesome and difficult work.

To evaluate the multidimensional Franck–Condon integrals quantitatively, a variety of theoretical methods [4–30] have been developed in the past several decades. One of these is based on the generating function approach of Sharp and Rosenstock [4] which is an extension of the method introduced by Hutchisson [5] for the diatomic case. This method has been further developed by Chen [6] and improved by Ervin et al. [7] in their application to the naphthyl radical. Very recently, Kikuchi et al. [8] derived a simpler form of the Sharp and Rosenstock general formula and applied it to SO_2 in the harmonic oscillator approximation. Another method based on the generating function approach is due to Ruhoff [9] who derived recursion relations for the calculation of multidimensional FCFs by generalizing Lerme's [10] procedure for two-dimensional FC overlap integrals. Also employing the generating function method, Islampour et al. [11] derived a closed-form multidimensional harmonic oscillator expression, where the FC overlap integrals were expressed as sums of products of Hermite polynomials. An alternative procedure, utilizing the recursion relations of Doctorov et al. [12,13] has been employed for a variety of molecules such as phenol [14,15], anthracene [16] and pyrazine [17]. In addition, two different methods for calculating the FC overlap integrals were developed by Faulkner and Richardson [18]. The central feature of their first method is a linear transformation of the normal coordinates in both the ground and excited electronic states in order to effectively remove the Duschinsky rotations. This was originally restricted to the case where either the initial or final vibrational wave function is the ground state, but Kulander later removed this restriction [19,20]. The second method of Faulkner and Richardson is based on a perturbation expansion of the vibrational wave functions of the excited electronic state in terms of the ground electronic state vibrational wave functions. Finally, Malmqvist and Forsberg [21] have expressed the FC matrix as the product of lower triangular and upper triangular matrices which are calculated from recursion formulas. On the other hand, Lin et al. [11,22–24] made a lot of contributions to calculations of multidimensional FC integrals. They obtained a closed-form formula

* Corresponding authors. Fax: +86 0553 3869 748 (J. Liang).
E-mail addresses: jliang@mail.ahnu.edu.cn (J. Liang), huangwei@aiofm.ac.cn (W. Huang).
[1] Laboratory of Atmospheric Physico-Chemistry, Anhui Institute of Optics and Fine Mechanics, Chinese Academy of Sciences, P.O. Box 1125, Hefei 230031, PR China.

0022-2852/$ - see front matter © 2013 Elsevier Inc. All rights reserved.
http://dx.doi.org/10.1016/j.jms.2013.02.009

of four-dimensional FC integrals on the basis of the contour integral of Hermite polynomials, and derived the analytical expressions for the calculation of the multidimensional Franck–Condon overlap integrals by using an addition theorem of Hermite polynomials.

Recently, Chang et al. [25–27] developed a simple method to calculate multidimensional FC integral of harmonic oscillators up to four dimensions including the Duschinsky effects. Some useful analytic formulae of multidimensional FC integrals were obtained and have been employed to study the photoelectron spectra of SO_2 and H_2O. However, the derived analytical expression for the calculation of the three-dimensional Franck–Condon overlap integrals was restricted to the case where either the initial or final vibrational wave function is the ground state. Another shortcoming of Chang's method is that they derived analytical expressions of multidimensional FC integrals and coefficient parameters by algebraic methods. In this work, we introduce the matrix expressions of some variables and coefficient parameters in the FC overlap integrals. Here, a more general analytical expression for the calculation of three-dimensional FC overlap integrals, with the inclusion of mode-mixing effects, is derived on the basis of matrix manipulation, similar to Chang's techniques [25–27]. A series of coefficient matrix relations between the coefficient parameters and the mode mixing transformation coefficients were found. Furthermore, the method for determining the coefficient parameter matrices was given by matrix manipulations. In addition, our approach has the advantages of being efficient and having no singular points [25]. Another advantage of a more general analytical expression for the calculation of the three-dimensional FC overlap integrals is that the FCF of any transition can be computed independently, without the necessity of storing FCFs for obtaining those of higher vibrational states as in the popular and well-documented recurrence approach [12,13]. Accordingly, our method can be applied to any distorted–rotated harmonic oscillators [25–30] and should be valuable in the studies of vibronic spectroscopy and nonradiative processes of molecules.

In order to test the validity of this new analytical expression formula, we calculated the photoelectron spectra of $PO_2^-(\widetilde{X}^1A_1)$ taking into account the mode mixing and hot band effects. The PO_2 radical is well known since it is easily generated by phosphorus–oxygen reactions, and it is also an important intermediate in phosphorus combustion chemistry [31–35]. The PO_2 spectrum of the $\widetilde{X}^2A_1$ ground state has been extensively investigated by various high-resolution spectroscopic methods [36–43]. Kawaguchi et al. [36] obtained an accurate ground state geometry and estimates of the lowest vibrational frequencies from far-infrared laser magnetic resonance (LMR) and microwave spectroscopy. The most accurate values obtained for the P–O bond length and the O–P–O bond angle are 1.4665 ± 0.0041 Å and 135.3 ± 0.8°, respectively. The estimated vibrational frequencies for the symmetric stretch (ω_1) and bend (ω_2) vibrational modes are 1090 and 377 cm^{-1}, respectively, from the centrifugal distortion constants. Laser induced fluorescence (LIF) and infrared absorption spectra observed by Hamilton and co-workers [37] also give similar ground state vibrational frequencies (ω_1=1117 cm^{-1} and ω_2 = 387 cm^{-1}). Lei et al. [43] later reported the laser fluorescence excitation spectra of PO_2 radicals in a jet-cooled molecular beam and they estimated vibrational intervals of 1075.4(50) and 397.3(43) cm^{-1} for the ω_1 and ω_2 vibrational modes. A few *ab initio* studies of the $\widetilde{X}^2A_1$ ground state of PO_2 have been reported in the literature [44–50]. In 1984, Lohr [44] performed seminal calculations of gas phase PO and PO_2 and their anions at the UHF, MP3 and CISD levels. Lohr and Boehm [45] later also calculated the vibrational frequencies of the $\widetilde{X}^2A_1$ state at the UHF/6-31G + d level. In 1989, Kabbadj and Lievin [46] calculated the equilibrium geometries, vibrational frequencies and adiabatic excitation energies for low-lying electronic states of PO_2 at the MCSCF and SCF levels including only valence electrons and all electrons, respectively, with small basis sets. In 1990, Jarrett-Spragne et al. [47] later reported the structure and vibrational spectra of PO_2 at the UHF/6-31G* level. In 1996, Buenker and co-workers [48] calculated the equilibrium geometry of the $\widetilde{X}^2A_1$ state by means of multireference single- and double-excitation configuration interaction (MRD-CI) calculations with a triple-zeta basis set plus two polarization d functions, as well as Rydberg orbitals. In 2002, Francisco [49] predicted the spectral and geometric parameters for PO_2 using the singles and doubles coupled cluster method, including a perturbational correction for connected triple excitations, CCSD(T), together with systematic sequences of correlation consistent basis sets. Lee et al. [50] later also carried out the geometry optimization and harmonic vibrational frequency calculations on some low-lying electronic states of PO_2 at the CIS, CASSCF, MP2, and RCCSD(T) levels with various standard basis sets of at least valence triple-ζ quality.

The corresponding negative ion (PO_2^-) is one of the possible anionic species occurring in oxidations of phosphorous compounds [51]. Research of the spectrum and dynamics of the PO_2^- anion is, however, comparatively scarce both theoretically and experimentally. Spectroscopic studies of PO_2^- have been limited to the solid phase: Geometries and vibrational frequencies of PO_2^- in a potassium chloride crystal have been obtained from spectroscopic and optically detected magnetic resonance studies by Francis and co-workers [52]. Prior to 1996, the gas phase anion of OPO was not known, although it has been generated as an impurity center in alkali halide crystals. In 1996, Xu et al. [53] reported the first gas phase photoelectron spectrum (PES) of PO_2^- anion. An electron affinity value of 3.42 ± 0.01 eV was reported from the experiments for PO_2. Additionally, they also determined the P–O bond length [r(O–P)=1.50 ± 0.01 Å] and the O–P–O bending angle ($\angle$(O–P–O)=120.0 ± 0.1°) for PO_2^- by fitting simulated spectrum to experimental. Nevertheless, they did not theoretically investigate how the overlap of the hot bands with the cold ones results in the final spectral pattern. On the other hand, Zhang et al. [54] calculated FCFs for the photodetachment of PO_2^- once again by using Sharp and Rosenstock's approach [4] taking into account the Duschinsky effect. They determined the P–O bond length (r(O–P) = 1.504 ± 0.005 Å) and the O–P–O bending angle ($\angle$(O–P–O) = 119.0 ± 0.2°) by an iterative FC analysis on Xu and co-workers' PES of PO_2^-. However, Zhang et al. completely ignored hot bands in the FCF calculations due to their weak signals, albeit some were observed and identified by Xu et al. [53]. Here we further investigate the $PO_2(\widetilde{X}^2A_1) - PO_2^-(\widetilde{X}^1A^1)$ photodetachment process. In this study, we simulated the PES of PO_2^- including contributions from both the 'cold' and 'hot' bands under the influence of the Duschinsky mode mixing effect on the basis of a more general analytical expression for the calculation of the three-dimensional Franck–Condon overlap integrals derived by us. In addition, an 'irregular spacing' [53] observed in the experimental photoelectron spectrum of PO_2^- is interpreted. Furthermore, employing the iterative Franck–Condon analysis procedure in the spectral simulation, the more reliable equilibrium geometries of the $\widetilde{X}^1A_1$ state of PO_2^- can be determined.

In the following section, we present a general formula of Franck–Condon overlap integral for three-dimensional harmonic oscillators. Then, Section 3 presents the results of equilibrium structures, vibrational frequencies and spectral simulation. The significance of the research findings is also discussed. Finally, Section 4 draws the conclusions.

2. Theory

2.1. General analytic expression for three-dimensional Franck–Condon integral

Upon an electronic transition, the wavefunction of three-dimensional harmonic oscillators in the $|v_1'v_2'v_3'\rangle$ vibrational state

of the initial electronic state and in the $|\upsilon_1\upsilon_2\upsilon_3\rangle$ vibrational state of the final electronic state can be expressed as, respectively,

$$|\upsilon_1'\upsilon_2'\upsilon_3'\rangle = \prod_{i=1}^{3} N_{\upsilon_i'} H_{\upsilon_i'}\left(\sqrt{\alpha_i'}Q_i'\right)\exp\left(-\frac{1}{2}\alpha_i' Q_i'^2\right) \tag{1}$$

and

$$|\upsilon_1\upsilon_2\upsilon_3\rangle = \prod_{i=1}^{3} N_{\upsilon_i} H_{\upsilon_i}(\sqrt{\alpha_i}Q_i)\exp\left(-\frac{1}{2}\alpha_i Q_i^2\right) \tag{2}$$

where υ_i' and υ_i (i = 1,2,3) are vibrational quantum numbers, $H_{\upsilon_i'}(x)$ and $H_{\upsilon_i}(x)$ are the Hermite polynomial, and the normalization constant,

$$N_{\upsilon_i'} = \left(\frac{\sqrt{\alpha_i'}}{2^{\upsilon_i'}\upsilon_i'!\sqrt{\pi}}\right)^{1/2} \quad \text{and } N_{\upsilon_i} = \left(\frac{\sqrt{\alpha_i}}{2^{\upsilon_i}\upsilon_i!\sqrt{\pi}}\right)^{1/2} \tag{3}$$

$$\text{with} \quad \alpha_i' = \frac{\omega_i'}{\hbar} \quad \text{and } \alpha_i = \frac{\omega_i}{\hbar} \tag{4}$$

where ω_i' and ω_i are the angular frequency of the ith mode for the initial electronic state and the final electronic state, respectively. It follows that the Franck–Condon vibrational overlap integral between $|\upsilon_1\upsilon_2\ \upsilon_3\rangle$ and $|\upsilon_1'\upsilon_2'\upsilon_3'\rangle$ states is

$$\begin{aligned}\langle\upsilon_1\upsilon_2\upsilon_3|\upsilon_1'\upsilon_2'\upsilon_3'\rangle = N\int_{-\infty}^{\infty}\int_{-\infty}^{\infty}\int_{-\infty}^{\infty} & H_{\upsilon_1'}(\sqrt{\alpha_1'}Q_1')H_{\upsilon_2'}\left(\sqrt{\alpha_2'}Q_2'\right)\\ & \times H_{\upsilon_3'}\left(\sqrt{\alpha_3'}Q_3'\right)\times H_{\upsilon_1}(\sqrt{\alpha_1}Q_1)H_{\upsilon_2}(\sqrt{\alpha_2}Q_2)\\ & \times H_{\upsilon_3}(\sqrt{\alpha_3}Q_3)\times\exp\left[-\left(\alpha_1'Q_1'^2+\alpha_2'Q_2'^2+\alpha_3'Q_3'^2\right.\right.\\ & \left.\left.+\alpha_1Q_1^2+\alpha_2Q_2^2+\alpha_3Q_3^2\right)/2\right]dQ_1dQ_2dQ_3\end{aligned} \tag{5}$$

where

$$N = \frac{1}{\pi^{3/2}}\left(\frac{\sqrt{\alpha_1\alpha_2\alpha_3\alpha_1'\alpha_2'\alpha_3'}}{2^{\upsilon_1+\upsilon_2+\upsilon_3+\upsilon_1'+\upsilon_2'+\upsilon_3'}\upsilon_1!\upsilon_2!\upsilon_3!\upsilon_1'!\upsilon_2'!\upsilon_3'!}\right)^{1/2} \tag{6}$$

An exact expression of FC integral for the vibronic transition $|\upsilon_1\upsilon_2\upsilon_3\rangle \leftarrow |\upsilon_1'\upsilon_2'\upsilon_3'\rangle$, will be derived in detail. When the Duschinsky effect must be taken into account, the normal coordinates $\mathbf{Q}'$ of the initial state ($|\upsilon_1'\upsilon_2'\upsilon_3'\rangle$) are related to those $\mathbf{Q}$ of the final state ($|\upsilon_1\upsilon_2\upsilon_3\rangle$) by

$$\mathbf{Q}' = \mathbf{JQ} + \mathbf{K} \tag{7}$$

where $\mathbf{J}$ is a 3×3 constant orthogonal matrix and $\mathbf{K}$ is a three-dimensional vector whose components are the changes in the nuclear equilibrium positions from the initial to final states. Upon substituting Eq. (7) into Eq. (5), expanding, and regrouping, we obtain

$$\begin{aligned}\langle\upsilon_1\upsilon_2\upsilon_3|\upsilon_1'\upsilon_2'\upsilon_3'\rangle = \exp\left(-\frac{1}{2}\mathbf{K}^+\mathbf{\Gamma}'\mathbf{K}\right)N\int_{-\infty}^{\infty}\int_{-\infty}^{\infty} & \\ \times\int_{-\infty}^{\infty} H_{\upsilon_1'}\left(\sqrt{\alpha_1'}Q_1'\right)H_{\upsilon_2'}\left(\sqrt{\alpha_2'}Q_2'\right) & \\ \times H_{\upsilon_3'}\left(\sqrt{\alpha_3'}Q_3'\right)H_{\upsilon_1}(\sqrt{\alpha_1}Q_1)H_{\upsilon_2}(\sqrt{\alpha_2}Q_2)H_{\upsilon_3}(\sqrt{\alpha_3}Q_3) & \\ \times\exp[-\mathbf{Q}^+\mathbf{J}'\mathbf{Q}-\mathbf{Q}^+\mathbf{W}]dQ_1\,dQ_2\,dQ_3 & \end{aligned} \tag{8}$$

where $\mathbf{\Gamma}'$ is a 3×3 diagonal matrix of reduced frequency $\omega_i'/\hbar$, and $^+$ indicates the Hermitian conjugate (which is, for a real matrix, the transpose), and a column vector

$$\mathbf{W} = \mathbf{J}^+\mathbf{\Gamma}'\ \mathbf{K} \tag{9}$$

and a 3×3 symmetric matrix

$$\mathbf{J}' = \frac{1}{2}(\mathbf{J}^+\mathbf{\Gamma}'\mathbf{J}+\mathbf{\Gamma}) \tag{10}$$

The exponent factor in the integrand in Eq. (8) is quadratic in $\mathbf{Q}$. Completing the square is accomplished by use of the transformation matrix $\mathbf{V}$ in the expression

$$\mathbf{Q} = \mathbf{VX}' \tag{11}$$

where $\mathbf{V}$ is chosen to satisfy the det$\mathbf{V}$ = 1 and yield the diagonal matrix $\mathbf{A}$, i.e.

$$\mathbf{V}^+\mathbf{J}'\mathbf{V} = \mathbf{A} \tag{12}$$

Substituting Eq. (11) into Eq. (8), and employing Eq. (12), we obtain

$$\begin{aligned}\langle\upsilon_1\upsilon_2\upsilon_3|\upsilon_1'\upsilon_2'\upsilon_3'\rangle = \exp\left(-\frac{1}{2}\mathbf{K}^+\mathbf{\Gamma}'\mathbf{K}\right)\exp(\mathbf{C}^+\mathbf{AC})N & \\ \times\int_{-\infty}^{\infty}\int_{-\infty}^{\infty}\int_{-\infty}^{\infty} H_{\upsilon_1'}\left(\sum_{k=1}^{3}a_{1k}'X_k+d_1'\right) & \\ \times H_{\upsilon_2'}\left(\sum_{k=1}^{3}a_{2k}'X_k+d_2'\right)\times H_{\upsilon_3'}\left(\sum_{k=1}^{3}a_{3k}'X_k+d_3'\right) & \\ \times H_{\upsilon_1}\left(\sum_{j=1}^{3}a_{1j}X_j+d_1\right)H_{\upsilon_2}\left(\sum_{j=1}^{3}a_{2j}X_j+d_2\right) & \\ \times H_{\upsilon_3}\left(\sum_{j=1}^{3}a_{3j}X_j+d_3\right) & \\ \times\exp(-\mathbf{X}^+\mathbf{AX})dX_1\,dX_2\,dX_3 & \end{aligned} \tag{13}$$

where $\mathbf{C} = \mathbf{A}^{-1}(\mathbf{V}^+\mathbf{W})/2$ is the three-dimensional column vector whose components are

$$C_i = \frac{(\mathbf{V}^+\mathbf{W})_i}{2A_i} \quad (i = 1,2,3) \tag{14}$$

and

$$\mathbf{X} = \mathbf{X}' + \mathbf{C} = \mathbf{V}^{-1}\mathbf{Q} + \mathbf{C} \tag{15}$$

In Eq. (13), the coefficients of Hermite polynomials are as follows:

$$\mathbf{a} = \mathbf{\Gamma}^{1/2}\mathbf{V}, \quad \text{i.e.} a_{ij} = \sqrt{\alpha_i}V_{ij} \quad (i,j = 1,2,3) \tag{16a}$$

$$\mathbf{a}' = \mathbf{\Gamma}'^{1/2}\mathbf{JV}, \quad \text{i.e. } a_{ik}' = \sum_{j=1}^{3}\sqrt{\alpha_i'}J_{ij}V_{jk} \quad (i,k = 1,2,3) \tag{16b}$$

$$\mathbf{d} = -\mathbf{\Gamma}^{1/2}\mathbf{VC}, \quad \text{i.e. } d_i = -\sqrt{\alpha_i}(\mathbf{VC})_i \quad (i = 1,2,3) \tag{16c}$$

$$\mathbf{d}' = -\mathbf{\Gamma}'^{1/2}(\mathbf{JVC}-\mathbf{K}), \quad \text{i.e.} d_i' = -\sqrt{\alpha_i'}(\mathbf{JVC}-\mathbf{K})_i \quad (i = 1,2,3) \tag{16d}$$

On the basis of expanding property of Hermite polynomials [55]:

$$\begin{aligned}H_{\upsilon_i}\left(\sum_{j=1}^{3}a_{ij}X_j+d_i\right) &= H_{\upsilon_i}(a_{i1}X_1+a_{i2}X_2+a_{i3}X_3+d_i)\\ &= \sum_{k_{i1}=0}^{\upsilon_i}\sum_{k_{i2}=0}^{\upsilon_i-k_{i1}}\sum_{k_{i3}=0}^{\upsilon_i-k_{i1}-k_{i2}}\binom{\upsilon_i}{k_{i1}}\binom{\upsilon_i-k_{i1}}{k_{i2}}\\ &\quad\times\binom{\upsilon_i-k_{i1}-k_{i2}}{k_{i3}}(a_{i1})^{k_{i1}}(a_{i2})^{k_{i2}}(a_{i3})^{k_{i3}}\\ &\quad\times H_{\upsilon_i-k_{i1}-k_{i2}-k_{i3}}(d_i)\times 2^{k_{i1}+k_{i2}+k_{i3}}\\ &\quad\times(X_1)^{k_{i1}}(X_2)^{k_{i2}}(X_3)^{k_{i3}}\end{aligned} \tag{17}$$

where $\binom{\upsilon_i}{k_1}$, $\binom{\upsilon_i-k_1}{k_2}$ and $\binom{\upsilon_i-k_1-k_2}{k_3}$ are coefficients. Inserting Eq. (17) into (13), one obtains

$$\begin{aligned}\langle \upsilon_1\upsilon_2\upsilon_3|\upsilon_1'\upsilon_2'\upsilon_3'\rangle &= \exp(-\frac{1}{2}\mathbf{K}^+\mathbf{\Gamma}'\mathbf{K})\exp(\mathbf{C}^+\mathbf{AC})N \\ &\times\prod_{i=1}^{3}\left[\sum_{k_{i1}'=0}^{\upsilon_i'}\sum_{k_{i2}'=0}^{\upsilon_i'-k_{i1}'}\sum_{k_{i3}'=0}^{\upsilon_i'-k_{i1}'-k_{i2}'}\binom{\upsilon_i'}{k_{i1}'}\binom{\upsilon_i'-k_{i1}'}{k_{i2}'}\binom{\upsilon_i'-k_{i1}'-k_{i2}'}{k_{i3}'}\right. \\ &\left.\times(a_{i1}')^{k_{i1}'}(a_{i2}')^{k_{i2}'}(a_{i3}')^{k_{i3}'}H_{\upsilon_i'-k_{1i}'-k_{i2}'-k_{i3}'}(d_i')\right] \\ &\times\prod_{i=1}^{3}\left[\sum_{k_{i1}=0}^{\upsilon_i}\sum_{k_{i2}=0}^{\upsilon_i-k_{i1}}\sum_{k_{i3}=0}^{\upsilon_i-k_{i1}-k_{i2}}\binom{\upsilon_i}{k_{i1}}\binom{\upsilon_i-k_{i1}}{k_{i2}}\binom{\upsilon_i-k_{i1}-k_{i2}}{k_{i3}}\right. \\ &\left.\times(a_{i1})^{k_{i1}}(a_{i2})^{k_{i2}}(a_{i3})^{k_{i3}}H_{\upsilon_i-k_{1i}-k_{i2}-k_{i3}}(d_i)\right] \\ &\times 2^{\sum_{i=1}^{3}(k_{i1}+k_{i1}')}\,2^{\sum_{i=1}^{3}(k_{i2}+k_{i2}')}\,2^{\sum_{i=1}^{3}(k_{i3}+k_{i3}')} \\ &\times\int_{-\infty}^{\infty}\int_{-\infty}^{\infty}\int_{-\infty}^{\infty}(X_1)^{\sum_{i=1}^{3}(k_{i1}+k_{i1}')}(X_2)^{\sum_{i=1}^{3}(k_{i2}+k_{i2}')} \\ &\times(X_3)^{\sum_{i=1}^{3}(k_{i3}+k_{i3}')}\times\exp(-\mathbf{X}^+\mathbf{AX})dX_1\,dX_2\,dX_3\end{aligned} \tag{18}$$

Up to this step, the three-dimensional vibrational overlap integral in Eq. (5) has reduced to a product of one-dimensional Gaussian integrals in Eq. (18). Gaussian integral can be evaluated by

$$\int_{-\infty}^{\infty}X^{2k}e^{-AX^2}dX = \frac{(2k-1)!!}{(2A)^k}\left(\frac{\pi}{A}\right)^{1/2} \tag{19}$$

where $(2k-1)!!$ is a double factorial. By means of the Gaussian integral formula (19), then the final closed form of the overlap integral is obtained

$$\begin{aligned}\langle \upsilon_1\upsilon_2\upsilon_3|\upsilon_1'\upsilon_2'\upsilon_3'\rangle &= \exp\left(-\frac{1}{2}\mathbf{K}^+\mathbf{\Gamma}'\mathbf{K}\right)\exp(\mathbf{C}^+\mathbf{AC})N \\ &\times\sum_{k_{11}'=0}^{\upsilon_1'}\sum_{k_{12}'=0}^{\upsilon_1'-k_{11}'}\sum_{k_{13}'=0}^{\upsilon_1'-k_{11}'-k_{12}'}\sum_{k_{21}'=0}^{\upsilon_2'}\sum_{k_{22}'=0}^{\upsilon_2'-k_{21}'}\sum_{k_{23}'=0}^{\upsilon_2'-k_{21}'-k_{22}'}\sum_{k_{31}'=0}^{\upsilon_3'}\sum_{k_{32}'=0}^{\upsilon_3'-k_{31}'} \\ &\times\sum_{k_{33}'=0}^{\upsilon_3'-k_{31}'-k_{32}'}\sum_{k_{11}=0}^{\upsilon_1}\sum_{k_{12}=0}^{\upsilon_1-k_{11}}\sum_{k_{13}=0}^{\upsilon_1-k_{11}-k_{12}}\sum_{k_{21}=0}^{\upsilon_2}\sum_{k_{22}=0}^{\upsilon_2-k_{21}}\sum_{k_{23}=0}^{\upsilon_2-k_{21}-k_{22}} \\ &\times\sum_{k_{31}=0}^{\upsilon_3}\sum_{k_{32}=0}^{\upsilon_3-k_{31}}\sum_{k_{33}=0}^{\upsilon_3-k_{31}-k_{32}} \\ &\times\left\{\prod_{i=1}^{3}\left[\binom{\upsilon_i'}{k_{i1}'}\binom{\upsilon_i'-k_{i1}'}{k_{i2}'}\binom{\upsilon_i'-k_{i1}'-k_{i2}'}{k_{i3}'}\right.\right. \\ &\times(a_{i1}')^{k_{i1}'}(a_{i2}')^{k_{i2}'}(a_{i3}')^{k_{i3}'}\times H_{\upsilon_i'-k_{i1}'-k_{i2}'-k_{i3}'}(d_i') \\ &\times\binom{\upsilon_i}{k_{i1}}\binom{\upsilon_i-k_{i1}}{k_{i2}}\binom{\upsilon_i-k_{i1}-k_{i2}}{k_{i3}} \\ &\left.\times(2a_{i1})^{k_{i1}}(2a_{i2})^{k_{i2}}(2a_{i3})^{k_{i3}}\times H_{\upsilon_i-k_{i1}-k_{i2}-k_{i3}}(d_i)\right] \\ &\times\frac{\left[\sum_{i=1}^{3}(k_{i1}+k_{i1}')-1\right]!!}{(2A_1)^{\frac{1}{2}\sum_{i=1}^{3}(k_{i1}+k_{i1}')}}\left(\frac{\pi}{A_1}\right)^{1/2}\frac{\left[\sum_{i=1}^{3}(k_{i2}+k_{i2}')-1\right]!!}{(2A_2)^{\frac{1}{2}\sum_{i=1}^{3}(k_{i2}+k_{i2}')}} \\ &\left.\times\left(\frac{\pi}{A_2}\right)^{1/2}\times\frac{\left[\sum_{i=1}^{3}(k_{i3}+k_{i3}')-1\right]!!}{(2A_3)^{\frac{1}{2}\sum_{i=1}^{3}(k_{i3}+k_{i3}')}}\left(\frac{\pi}{A_3}\right)^{1/2}\right\}\end{aligned} \tag{20}$$

with the constraints that $\sum_{i=1}^{3}(k_{i1}+k_{i1}')$, $\sum_{i=1}^{3}(k_{i2}+k_{i2}')$ and $\sum_{i=1}^{3}(k_{i3}+k_{i3}')$ are even. Furthermore, from Eq. (20) an exact formula of calculating the three-dimensional overlap integral for the vibronic transition $|\upsilon_1\upsilon_2\upsilon_3\rangle \leftarrow |000\rangle$, is given explicitly as:

$$\begin{aligned}\langle \upsilon_1\upsilon_2\upsilon_3|000\rangle &= \exp\left(-\frac{1}{2}\mathbf{K}^+\mathbf{\Gamma}'\mathbf{K}\right)\exp(\mathbf{C}^+\mathbf{AC})N \\ &\times\sum_{k_{11}=0}^{\upsilon_1}\sum_{k_{12}=0}^{\upsilon_1-k_{11}}\sum_{k_{13}=0}^{\upsilon_1-k_{11}-k_{12}}\sum_{k_{21}=0}^{\upsilon_2}\sum_{k_{22}=0}^{\upsilon_2-k_{21}}\sum_{k_{23}=0}^{\upsilon_2-k_{21}-k_{22}}\sum_{k_{31}=0}^{\upsilon_3}\sum_{k_{32}=0}^{\upsilon_3-k_{31}} \\ &\times\sum_{k_{33}=0}^{\upsilon_3-k_{31}-k_{32}}\left\{\prod_{i=1}^{3}\left[\times\binom{\upsilon_i}{k_{i1}}\binom{\upsilon_i-k_{i1}}{k_{i2}}\binom{\upsilon_i-k_{i1}-k_{i2}}{k_{i3}}\right.\right. \\ &\left.\times\left(2a_{i1}\right)^{k_{i1}}(2a_{i2})^{k_{i2}}(2a_{i3})^{k_{i3}}\times H_{\upsilon_i-k_{i1}-k_{i2}-k_{i3}}(d_i)\right] \\ &\times\frac{\frac{\left[\sum_{i=1}^{3}k_{i1}-1\right]!!}{(2A_1)^{\frac{1}{2}\sum_{i=1}^{3}k_{i1}}}\left(\frac{\pi}{A_1}\right)^{1/2}\frac{\left[\sum_{i=1}^{3}k_{i2}-1\right]!!}{(2A_2)^{\frac{1}{2}\sum_{i=1}^{3}k_{i2}}}\left(\frac{\pi}{A_2}\right)^{1/2}\left[\sum_{i=1}^{3}k_{i3}-1\right]!!}{(2A_3)^{\frac{1}{2}\sum_{i=1}^{3}k_{i3}}\left(\frac{\pi}{A_3}\right)^{1/2}}\Bigg\}\end{aligned} \tag{21}$$

with the constraints $\sum_{i=1}^{3}k_{i1}$, $\sum_{i=1}^{3}k_{i2}$ and $\sum_{i=1}^{3}k_{i3}$ all being even.

Finally, the Franck–Condon factors (FCFs) of three-dimensional harmonic oscillators including the Duschinsky effect can be evaluated by

$$\text{FCFs} = \left|\langle \upsilon_1\upsilon_2\upsilon_3|\upsilon_1'\upsilon_2'\upsilon_3'\rangle\right|^2 \tag{22}$$

Eq. (20) is exact for harmonic systems, no approximation whatsoever having been introduced in its derivation. This expression should be very useful for studying vibronic spectra and nonradiative processes of molecules.

2.2. Calculation method of constant coefficient matrices and vectors

Above, the new analytic expression for three-dimensional Franck–Condon integral is shown. Given the Duschinsky matrix **J** and the vector **K**, we can find matrix elements of other coefficient matrices and vectors such as the transformation matrix **V**, the diagonal matrix **A** and constant coefficient vector **C**. Firstly, from the transformation relation (15), i.e. $\mathbf{X} = \mathbf{V}^{-1}\mathbf{Q} + \mathbf{C}$, setting

$$\mathbf{V}^{-1} = \begin{bmatrix}1 & B_1 & B_2\\ 0 & 1 & B_3\\ 0 & 0 & 1\end{bmatrix} \tag{23}$$

Then its inverse matrix can be found

$$\mathbf{V} = \begin{bmatrix}1 & -B_1 & B_1B_3-B_2\\ 0 & 1 & -B_3\\ 0 & 0 & 1\end{bmatrix} \tag{24}$$

Here **V** satisfy det**V** = 1, and yield the diagonal matrix**A**. On the based of the matrix Eq. (12), i.e. $\mathbf{V}^+\mathbf{J}'\mathbf{V} = \mathbf{A}$, the matrix equation is given explicitly as

$$\begin{bmatrix}1 & 0 & 0\\ -B_1 & 1 & 0\\ B_1B_3-B_2 & -B_3 & 1\end{bmatrix}\begin{bmatrix}J_{11}' & J_{12}' & J_{13}'\\ J_{21}' & J_{22}' & J_{23}'\\ J_{31}' & J_{32}' & J_{33}'\end{bmatrix}\begin{bmatrix}1 & -B_1 & B_1B_3-B_2\\ 0 & 1 & -B_3\\ 0 & 0 & 1\end{bmatrix} = \begin{bmatrix}A_1 & 0 & 0\\ 0 & A_2 & 0\\ 0 & 0 & A_3\end{bmatrix} \tag{25}$$

By the matrix Eq. (25), one obtain

$$A_1 = J'_{11} \tag{26a}$$
$$B_1 = J'_{12}/J'_{11} \tag{26b}$$
$$B_2 = J'_{13}/J'_{11} \tag{26c}$$
$$A_2 = J'_{22} - J'^2_{12}/J'_{11} \tag{26d}$$
$$B_3 = (J'_{13} - J'_{12}J'_{13}/J'_{11})/\left(J'_{22} - J'^2_{12}/J'_{11}\right) \tag{26e}$$
$$A_3 = J'_{33} - J'^2_{13}/J'_{11} - (J'_{13} - J'_{12}J'_{13}/J'_{11})^2/\left(J'_{22} - J'^2_{12}/J'_{11}\right) \tag{26f}$$

In addition, by Eq. (14) the coefficient vector **C** can be determined from **V**, **A** and **W**, i.e.

$$C_1 = \left(\sum_{i=1}^{3}\alpha'_i J_{i1}K_i\right)/(2A_1) \tag{27a}$$
$$C_2 = \left(\sum_{i=1}^{3}\alpha'_i J_{i2}K_i - 2A_1B_1C_1\right)/(2A_2) \tag{27b}$$
$$C_3 = \left(\sum_{i=1}^{3}\alpha'_i J_{i3}K_i - 2A_1B_2C_1 - 2A_2B_3C_2\right)/(2A_3) \tag{27c}$$

By means of Eqs. (16a)–(16d), the coefficients of Hermite polynomials are obtained:

$$a_{11} = \sqrt{\alpha_1}, \quad a_{12} = -\sqrt{\alpha_1}B_1, \quad a_{13} = \sqrt{\alpha_1}(B_1B_3 - B_2) \tag{28a}$$
$$a_{21} = 0, \quad a_{22} = \sqrt{\alpha_2}, \quad a_{23} = -\sqrt{\alpha_2}B_3 \tag{28b}$$
$$a_{31} = 0, \quad a_{32} = 0, \quad a_{33} = \sqrt{\alpha_3} \tag{28c}$$

$$a'_{11} = \sqrt{\alpha'_1}J_{11}, \quad a'_{12} = \sqrt{\alpha'_1}(J_{12} - B_1J_{11}) \tag{29a}$$
$$a'_{13} = \sqrt{\alpha'_1}[J_{13} - B_3J_{12} + (B_1B_3 - B_2)J_{11}] \tag{29b}$$
$$a'_{21} = \sqrt{\alpha'_2}J_{21}, \quad a'_{22} = \sqrt{\alpha'_2}(J_{22} - B_1J_{21}) \tag{29c}$$
$$a'_{23} = \sqrt{\alpha'_2}[J_{23} - B_3J_{22} + (B_1B_3 - B_2)J_{21}] \tag{29d}$$
$$a'_{31} = \sqrt{\alpha'_3}J_{31}, \quad a'_{32} = \sqrt{\alpha'_3}(J_{32} - B_1J_{31}) \tag{29e}$$
$$a'_{33} = \sqrt{\alpha'_3}[J_{33} - B_3J_{32} + (B_1B_3 - B_2)J_{31}] \tag{29f}$$

$$d_1 = -\sqrt{\alpha_1}[C_1 - B_1C_2 + (B_1B_3 - B_2)C_3] \tag{30a}$$
$$d_2 = -\sqrt{\alpha_2}(C_2 - B_3C_3) \tag{30b}$$
$$d_3 = -\sqrt{\alpha_3}C_3 \tag{30c}$$

$$d'_1 = -\sqrt{\alpha'_1}\{C_1J_{11} + C_2(J_{12} - B_1J_{11}) + C_3[(B_1B_3 - B_2)J_{11} - B_3J_{12} + J_{13}] - K_1\} \tag{31a}$$

$$d'_2 = -\sqrt{\alpha'_2}\{C_1J_{21} + C_2(J_{22} - B_1J_{21}) + C_3[(B_1B_3 - B_2)J_{21} - B_3J_{22} + J_{23}] - K_2\} \tag{31b}$$

$$d'_3 = -\sqrt{\alpha'_3}\{C_1J_{31} + C_2(J_{32} - B_1J_{31}) + C_3[(B_1B_3 - B_2)J_{31} - B_3J_{32} + J_{33}] - K_3\} \tag{31c}$$

Furthermore, it can be easily proven that our formula (21) is identical to the formula (A4)-(A7) reported in Ref. [27] by Chang. Note that $a_{21} = 0$, $a_{31} = 0$ and $a_{32} = 0$ in Eq. (28), so Eq. (21) is simplified as

$$\begin{aligned}\langle \upsilon_1\upsilon_2\upsilon_3|000\rangle = {} & \exp\left(-\frac{1}{2}\mathbf{K}^+\mathbf{\Gamma}'\mathbf{K}\right)\exp(\mathbf{C}^+\mathbf{A}\mathbf{C})N \\ & \times \sum_{k_{11}=0}^{\upsilon_1}\sum_{k_{12}=0}^{\upsilon_1-k_{11}}\sum_{k_{13}=0}^{\upsilon_1-k_{11}-k_{12}}\sum_{k_{22}=0}^{\upsilon_2}\sum_{k_{23}=0}^{\upsilon_2-k_{22}}\sum_{k_{33}=0}^{\upsilon_3}\left\{\binom{\upsilon_1}{k_{11}}\binom{\upsilon_1-k_{11}}{k_{12}}\right. \\ & \times \binom{\upsilon_1-k_{11}-k_{12}}{k_{13}}\binom{\upsilon_2}{k_{22}}\binom{\upsilon_2-k_{22}}{k_{23}}\binom{\upsilon_3}{k_{33}} \\ & \times (2a_{11})^{k_{11}}(2a_{12})^{k_{12}}(2a_{13})^{k_{13}}(2a_{22})^{k_{22}}(2a_{23})^{k_{23}}(2a_{33})^{k_{33}} \\ & \times H_{\upsilon_1-k_{11}-k_{12}-k_{13}}(d_1)H_{\upsilon_2-k_{22}-k_{23}}(d_2)H_{\upsilon_3-k_{33}}(d_3)\frac{[k_{11}-1]!!}{(2A_1)^{k_{11}/2}}\left(\frac{\pi}{A_1}\right)^{1/2} \\ & \left.\times \frac{[k_{12}+k_{22}-1]!!}{(2A_2)^{(k_{12}+k_{22})/2}}\left(\frac{\pi}{A_2}\right)^{1/2}\frac{[k_{13}+k_{23}+k_{23}-1]!!}{(2A_3)^{(k_{13}+k_{23}+k_{23})/2}}\left(\frac{\pi}{A_3}\right)^{1/2}\right\}\end{aligned} \tag{32}$$

with the constraints k_{11}, $(k_{12} + k_{22})$ and $k_{13} + k_{23} + k_{23}$ all being even. Eq. (32) is completely consistent with Eqs. (A4)-(A7) reported in Ref. [27]. Hence, we conclude that Eq. (20) obtained in this work is a

Table 1
Summary of some computed and experimental geometric parameters and vibrational frequencies (cm^{-1}) for the $\widetilde{X}^2A_1$ state of PO_2 obtained at different levels of theory.

Method	r(O–P) (Å)	∠(O–P–O) (°)	ω_1 (a_1)	ω_2 (a_1)	ω_3 (b_2)
B2PLYP/aug-cc-pVDZ	1.519	133.82	985.0	367.2	1270.1
B2PLYP/aug-cc-pVTZ	1.4863	134.13	1046.1	384.1	1332.0
CCSD(T)/aug-cc-pVDZ[d]	1.5230	134.02	977.8	364.9	1241.2
CCSD(T)/aug-cc-pVTZ[d]	1.4854	134.64	1054.8	383.4	1326.1
CCSD(T)/aug-cc-pVQZ[d]	1.4745	134.83	1072.3	390.4	1348.5
CCSD(T)/aug-cc-pV5Z	1.4686	135.25	1081.2	391.6	1362.2
MRD-CI/TZ + 2d + R[a]	1.464	135.14	1052	389	1338
B3LYP/6-311 + G (2d,p)[b]	1.4762	134.2861	1059.4	381.9	1305.1
B3LYP/6-311 + G (d,p)[b]	1.4851	133.6917	1049.1	375.7	1285.6
CCSD/6-311 + G (2d,p)[b]	1.4686	135.1822	1089.0	402.7	1345.9
QCISD(T)/6-311 + G (2d,p)[b]	1.4723	135.0226	1069.3	399.1	1326.2
MP2/6-311 + G (2d,p)[b]	1.4806	136.7967	1076.2	398.5	1477.4
MP2/6-311 + G (3df)[c]	1.478	136.6	1085	403	1486
CCSD(T)(FC)/cc-pVDZ[d]	1.515	133.5	1002	371	1283
CCSD(T)(FC)/cc-pVTZ[d]	1.482	134.6	1066	387	1342
CCSD(T)(FC)/cc-pVQZ[d]	1.473	134.9	1076	391	1353
Expt. (LMR, microwave)[e]	1.4665 ± 0.0041	135.3 ± 0.8	1090	377	
Expt. (LIF)[f]			1117 ± 20	387 ± 20	
Expt. (LMR LF)[g]			1076 ± 12	397 ± 12	
Expt. (PES)[h]			1070	380	
Expt. (DL)[i]					1327.53

[a] Ref. [48].
[b] Ref. [54].
[c] Ref. [50].
[d] Ref. [49].
[e] Ref. [36].
[f] Ref. [37].
[g] Ref. [43].
[h] Ref. [53].
[i] Ref. [40].

Table 2
Summary of some computed and experimental geometric parameters and vibrational frequencies (cm^{-1}) for the $\widetilde{X}^1A_1$ state of PO_2^- obtained at different levels of theory.

Method	r(P–O) (Å)	∠(O–P–O) (°)	ω_1 (a_1)	ω_2 (a_1)	ω_3 (b_2)
B2PLYP/aug-cc-PVDZ	1.5570	117.86	966.8	422.1	1089.7
B3LYP/cc-pVQZ	1.5077	118.53	1064.8	461.8	1210.2
CCSD(T)/aug-cc-pVDZ[b]	1.5606	118.04	969.9	422.9	1095.6
CCSD(T)/aug-cc-pVTZ[b]	1.5190	118.67	1045.2	447.6	1191.4
CCSD(T)/aug-cc-pVQZ[b]	1.5080	118.90	1060.3	454.0	1211.5
CCSD(T)/aug-cc-pV5Z	1.5024	119.23	956.4	446.3	1113.0
QCISD(T)(FC)/cc-pVQZ	1.5078	118.83	1064.3	461.0	1220.6
B3LYP/6-311 + G (2d,p)[a]	1.5108	119.09	1042.7	449.2	1187.3
B3LYP/6-311G (2d,p)[a]	1.5082	118.7187	1062.9	463.9	1212.7
QCISD(T)(FC)/6-311 + G (2d,p)[a]	1.5068	119.3108	1059.71	461.8	1207.8
CCSD(T)(FC)/6-311 + G (2d,p)[a]	1.5038	119.4375	1075.4	467.7	1225.8
CCSD(T)/cc-pVDZ[b]	1.548	117.9	1008	459	1155
CCSD(T)/cc-pVTZ[b]	1.514	118.8	1068	463	1227
CCSD(T)/cc-pVQZ[b]	1.506	118.9	1072	463	1227
Expt. (IR)[c]					1198.6
Expt. (PES)[d]	1.50 ± 0.01	120 ± 0.1		520	
IFCA	1.495 ± 0.005	119.5 ± 0.5			

[a] Ref. [54].
[b] Ref. [49].
[c] Ref. [51].
[d] Ref. [53].

general analytical expression for calculation of three-dimensional Franck–Condon integral, while the formula reported in Ref. [27] by Chang which is equivalent to Eq. (32) is only one kind of especial cases for calculations of three-dimensional Franck–Condon integral which can be obtained very easily from above Eq. (20).

3. Example for an application

3.1. Equilibrium structures and vibrational frequencies

Employing the Gaussian**09** suite of programs [56], geometry optimization and harmonic vibrational frequency calculations were carried out on the $\widetilde{X}^2A_1$ states of the neutral molecule PO_2, and $\widetilde{X}^1A_1$ state of the negative ion PO_2^- by using the density functional theory (B2PLYP functional) and the coupled cluster singles and doubles with perturbative triples [CCSD(T)] method with different basis sets up to aug-cc-pV5Z. Closed and open shell molecules were computed by restricted and unrestricted methods, respectively. Computed results obtained from the present investigation are summarized in Tables 1 and 2 together with available calculated and experimental data for comparison. The bending vibration is denoted ω_2, according to the convention for triatomic molecules.

From Table 1, for the state $\widetilde{X}^2A_1$ of PO_2, the computed bond lengths and angles obtained at different levels of calculation seem to be highly consistent. For r(O–P) and ∠(O–P–O), the largest deviations between calculated and experimental bond lengths and angles are less than 0.0565 Å and 1.5°, respectively (see Table 1). Based on the *ab initio* techniques at the CCSD(T)/aug-cc-pV5Z level, the estimated values are 1.4686 Å and 135.25° for r(O–P) and ∠(O–P–O). The differences between calculated and experimental values are only 0.002 Å and 0.05° for r(O–P) and ∠(O–P–O), respectively. The theoretical vibrational frequencies at all levels match reasonably well with the observed data. This suggests that the use of the *ab initio*force constants in the proposed iterative FC analysis scheme should give reliable parameters of PO_2^- in the $\widetilde{X}^1A_1$ state. Both the optimized geometric parameters and the vibrational frequencies calculated at CCSD(T)/aug-cc-pV5Z level gave the better agreement with the corresponding available experimental values, and were therefore utilized in subsequent iterative FC analyses and spectral simulation.

For the state $\widetilde{X}^1A_1$ of PO_2^-, the computed bond lengths and angles obtained at different levels of calculation seem to be highly consistent. However, the computed bond lengths and angles of

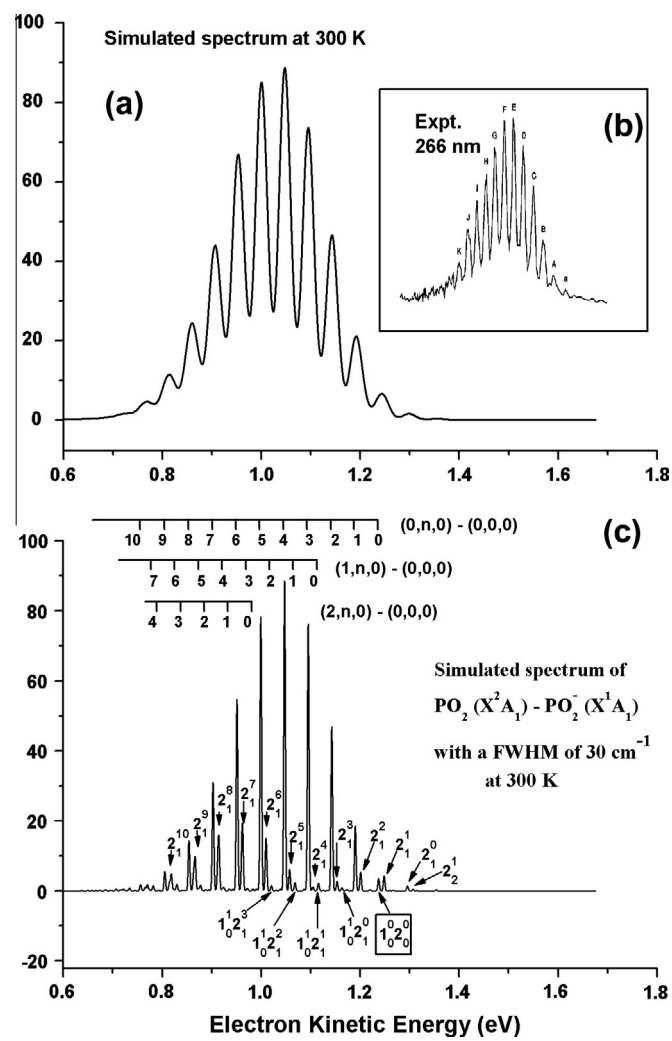

Fig. 1. $\widetilde{X}^2A_1 - \widetilde{X}^1A_1$ photodetachment spectrum of PO_2^- at a Boltzmann vibrational temperature of 300 K. (a) The spectrum from the present calculations (top trace, FWHM = 200 cm^{-1}), and (b) the experimental photodetachment spectrum from Ref. [53] (top right), and (c) the simulated photodetachment spectrum with their vibrational assignments (bottom trace, FWHM = 30 cm^{-1}).

the $\widetilde{X}^1A_1$ state appear to be sensitive to the basis sets. From Table 2, it can be seen that the computed bond angles converge towards larger values while bond lengths towards smaller ones when the basis sets are improved from aug-cc-pVDZ to aug-cc-pV5Z. Because no experimental geometric parameters were obtained for comparison, it is expected that the geometrical parameters acquired at the higher levels with large basis sets should be more reliable. The estimated values based on the *ab initio* techniques at the CCSD(T)/aug-cc-pV5Z level, are 1.5024 Å and 119.23° for r(O–P), and ∠(O–P–O), respectively. Regarding the computed vibrational frequencies, for the state $\widetilde{X}^1A_1$ of PO_2^-, the values obtained at the various levels are reasonably consistent. For the bending mode ω_2, and asymmetrical stretching mode ω_3, the differences between estimated at the CCSD(T)/aug-cc-pV5Z level and experimental ones are 74 cm^{-1} and 85 cm^{-1}, respectively. Discrepancies between experimental values and computed ones are mainly due to anharmonicity effect not to be included in the theoretical calculations. The CCSD(T)/aug-cc-pV5Z results are the best overall agreement to the corresponding available experimental and other theoretical values, and were therefore utilized in subsequent iterative FC analyses and spectral simulations.

3.2. Franck–Condon simulations

The Duschinsky matrix and displacement vector between the ground states of PO_2^- and PO_2 calculated at the CCSD(T)/aug-cc-pV5Z theory level are as follows:

$$\mathbf{J} = \begin{bmatrix} 0.97 & -0.20 & 0 \\ 0.20 & 0.97 & 0 \\ 0 & 0 & 0.997 \end{bmatrix}, \quad \mathbf{K} = \begin{bmatrix} -0.27 \\ 0.83 \\ 0 \end{bmatrix} \tag{33}$$

where **K** is in units of amu$^{1/2}$Å. Examination of **J**, which describes the mixing of normal modes, reveals that each one of the two a_1 modes of PO_2^-, maps onto a linear combination of the two a_1 modes of PO_2. Note that each column in **J** is normalized, the sum of the squares of the mixing coefficients adding up to unity within rounding errors. Eq. (33) shows that there is some, albeit not large ($J_{12} = -0.2$, $J_{21} = 0.2$), Duschinsky effect between $\omega_1(a_1)$ and $\omega_2(a_1)$ vibrational modes, whereas $\omega_3(b_2)$ is uncoupled from $\omega_1(a_1)$ and $\omega_2(a_1)$ due to different symmetry. **K** is a measure of the change in equilibrium geometry upon detachment along each normal mode of the negative ion. The normal coordinate displacements from

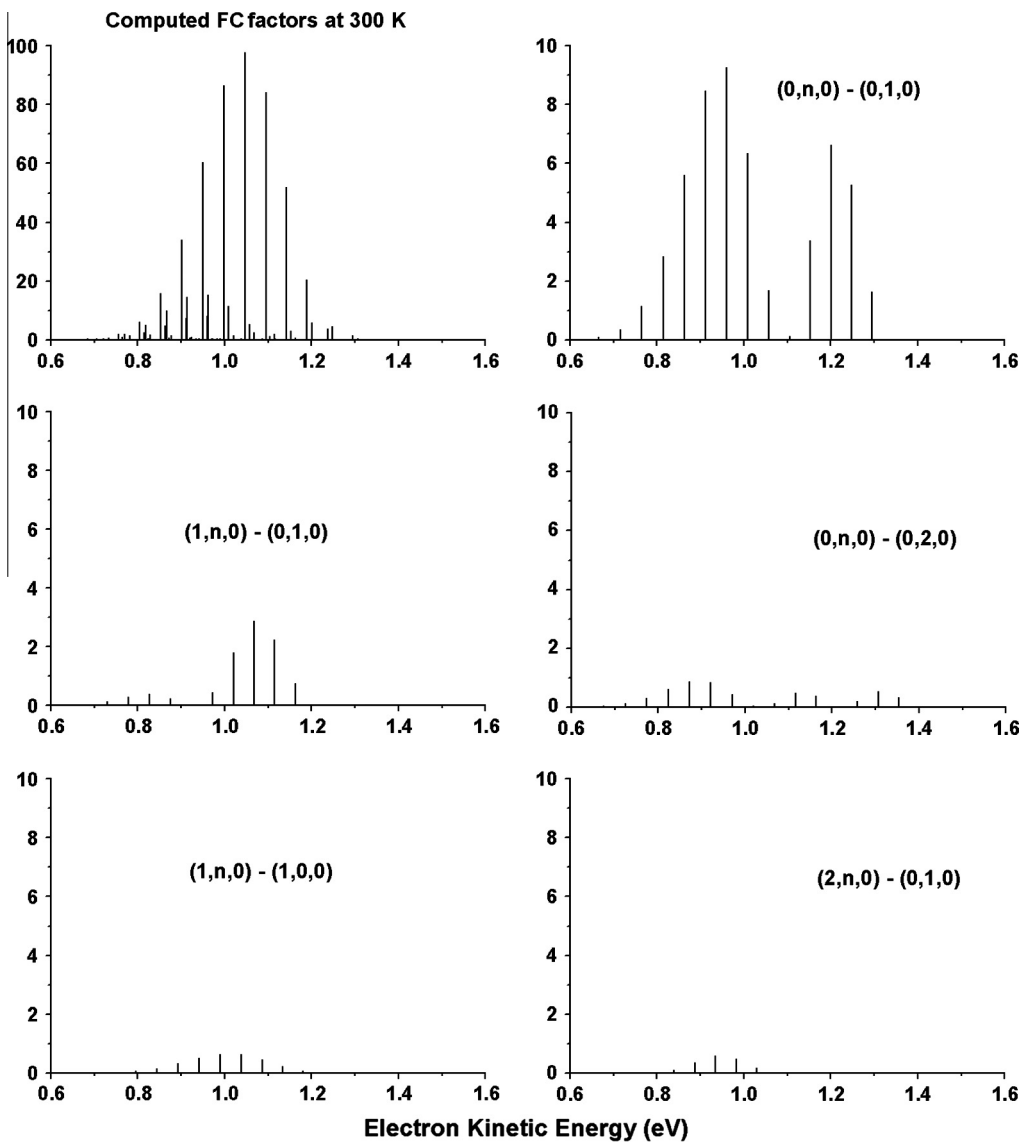

Fig. 2. The computed relative intensities with a Boltzmann vibrational temperature of 300 K (top left), and the computed relative intensities of some major 'hot' band series with their vibrational assignments (in order to show more clearly the relatively weak 'hot' band series, the *y*-axes for individual 'hot' bands have different scales from that at top left).

the anion to the neutral are $\Delta Q_1 = -0.27$, $\Delta Q_2 = 0.83$, which correspond to a bond length decrease and a bond angle increase, respectively. Meanwhile, one can observe that ΔQ_2 is about three times of ΔQ_1, stemming from the large change of the bending angle, and therefore a long progression of the bending vibration (ω_2) transitions is expected.

Using data obtained from the CCSD(T)/aug-cc-pV5Z calculations, the photodetachment spectrum of PO_2^- has also been simulated at a Boltzmann vibrational temperature of 300 K, as shown in Fig. 1a, with experimental one (from Ref. [53]) shown in Fig. 1b. This simulation has employed a FWHM of 220 cm^{-1}, because an experimental resolution of 25 meV (about 220 cm^{-1}) was given in Ref. [53]. It was seen the vibrational structure simulated with a FWHM of 220 cm^{-1} as shown in Fig. 1a matches very well with the 266 nm laser experimental spectrum of Ref. [53] in Fig. 1b.

Simulated photoelectron spectra of the $PO_2(\widetilde{X}^2A_1) - PO_2^-(\widetilde{X}^1A_1)$ photodetachment with a FWHM of 30 cm^{-1} and a Boltzmann vibrational temperature of 300 K are shown in Fig. 1c. Vibrational assignments for the symmetric stretching ω_1 and bending ω_2 modes of the neutral molecule PO_2 are also provided in Fig. 1c, respectively, with the labels $(0,n,0)$ – $(0,0,0)$, $(1,n,0)$ – $(0,0,0)$ and $(2,n,0)$ – $(0,0,0)$ corresponding to the $(\omega_1,\omega_2,0)$ – $(0,0,0)$ transition. The computed relative intensities of the major 'hot' bands are identified and their assignments are given in Fig. 1c, with the label 2_2^1corresponding to the $(0,1,0)$ – $(0,2,0)$, 2_1^n $(n = 0,\ldots,10)$ corresponding to the $(0,n,0)$ – $(0,1,0)$ and $1_0^1 2_1^n$ $(n = 0,\ldots,3)$ corresponding to the $(1,n,0)$ – $(0,1,0)$ transitions. From the harmonic calculation, it was found that the FCFs for transitions involving the asymmetric stretching mode ω_3 are negligibly small and therefore the ω_3 mode is not included in the assignments.

Since it is not uncommon for vibrationally 'hot' anions to be produced in the anion source used in a typical photodetachment experiment as that of Ref. [53], the computed relative intensities of the major 'hot' band series and their assignments obtained at a Boltzmann vibrational temperature of 300 K are given in Fig. 2. Calculations of relative intensities for hot bands provide detailed insights into the PES of PO_2^-. Xu et al. [53] experimentally identified only one hot band peak 'a' (i.e., 2_1^0), but did not observe other transitions (e.g., 2_2^0, 1_1^0 and 2_2^1, etc.). Fig. 2 demonstrates that the signal of 2_2^0 is too weak to be detectable because of its small relative intensity, as are the other missing bands (not shown).

Our finding is important in the assignment of the experimental PES of PO_2^-. Xu and co-workers [53] found that the peaks *G* and *H* (see Fig. 1b), which are separated by only 330 cm^{-1}, have irregular ω_2 spacing, and interpreted that there might be more than one active vibrational mode. Nevertheless, the present study shows that hot bands also contribute to the 'irregular spacing' with some extent. From Fig. 2, it was found that the relative intensities for transitions 2_1^7 and 2_1^8 are far larger than 2_1^0 and are almost equal to the combination bands $1_0^1 2_0^3$ and $1_0^1 2_0^4$, respectively. The peak G consists of $2_0^6 1_0^1 2_0^3$ and 2_1^7. The peak *H* consists of $2_0^7 1_0^1 2_0^4$ and 2_1^8. As a result, the peaks *G* and *H* are separated by only 330 cm^{-1} in the experimental PES of PO_2^-.

The variations of geometries of the molecule between the electronic states using the iterative FC analysis method [6] would yield better matches between the simulated and observed spectra than that obtained with the *ab initio* geometries. Since the experimental geometry of the $\widetilde{X}^2A_1$ state of PO_2 is available, the IFCA method was carried out on the $\widetilde{X}^1A_1$ state of PO_2^-. By fitting simulated spectrum to experimental, the best IFCA bond length *r*(O–P) and bond angle ∠(O–P–O) obtained for the ground state $\widetilde{X}^1A_1$ state of PO_2^-, employing the CCSD(T)/aug-cc-pV5Z force constants, are 1.495 ± 0.005 Å and 119.5 ± 0.5°, respectively. This result is consistent with the results obtained by Xu et al. and *ab initio* and DFT calculations (see Table 2).

4. Conclusion

We derived a general formula of the three-dimensional Franck–Condon overlap integrals for three-dimensional harmonic oscillators by expanding Hermite polynomials and solving Gaussian integrals. Furthermore, the PES of PO_2^- was elucidated in detail and the role of Duschinsky effects and hot bands were clarified. In the case of the photoelectron spectrum of the $PO_2(\widetilde{X}^2A_1)$ – $PO_2^-(\widetilde{X}^1A_1)$ detachment, it seems that the harmonic model is reasonably adequate. The rather reliable bond length *r*(O–P) and bond angle ∠(O-P–O) were obtained, through the IFCA procedure. Based on the sensitivity of the relative intensities on the variation of the bond length and bond angle, the uncertainties in the *r*(OP) and ∠(OPO) are probably around ±0.005 Å and ±0.5°, respectively.

Acknowledgments

This work was supported by the National Nature Science Foundation of China (No. 21273009, 21073196, 21133008), the Nature Science Foundation of the Education Committee of Anhui (No. KJ2009A131), the Program for Innovative Research Team in Anhui Normal University, and the Doctoral Research Foundation of Anhui Normal University (No. 750706).

References

[1] J. Frank, Trans. Faraday Soc. 21 (1925) 536–542.
[2] E.U. Condon, Phys. Rev. 32 (1928) 858–872.
[3] F. Duschinsky, Acta Physicochim. URSS 7 (1937) 551–566.
[4] T.E. Sharp, H.M. Rosenstock, J. Chem. Phys. 41 (1964) 3453–3463.
[5] E. Hutchisson, Phys. Rev. 36 (1930) 410–420.
[6] P. Chen, in: C.-Y. Ng, T. Baer, I. Powis (Eds.), Unimolecular and Bimolecular Reaction Dynamics, Wiley, Chichester, 1994, p. 371.
[7] K.M. Ervin, T.M. Ramond, G.E. Davico, R.L. Schwartz, S.M. Casey, W.C. Lineberger, J. Phys. Chem. A 105 (2001) 10822–10831.
[8] H. Kikuchi, M. Kubo, N. Watanabe, H. Suzuki, J. Chem. Phys. 119 (2003) 729–736.
[9] P.T. Ruhoff, Chem. Phys. 186 (1994) 355–374.
[10] J. Lerme, Chem. Phys. 145 (1990) 67–88.
[11] R. Islampour, M. Dehestani, S.H. Lin, J. Mol. Spectrosc. 194 (1999) 179–184.
[12] E.V. Doctorov, I.A. Malkin, V.I. Man'ko, J. Mol. Spectrosc. 56 (1975) 1–20.
[13] E.V. Doctorov, I.A. Malkin, V.I. Man'ko, J. Mol. Spectrosc. 64 (1977) 302–326.
[14] P.R. Callis, J.T. Vivian, L.S. Slater, Chem. Phys. Lett. 244 (1995) 53–58.
[15] S. Schumm, M. Gerhards, K. Kleinermanns, J. Phys. Chem. A 104 (2000) 10648–10655.
[16] D. Gruner, A. Nguyen, P. Brumer, J. Chem. Phys. 101 (1994) 10366–10381.
[17] R. Berger, C. Fischer, M. Klessinger, J. Phys. Chem. A102 (1998) 7157–7167.
[18] T.R. Faulkner, F.S. Richardson, J. Chem. Phys. 70 (1979) 1201–1213.
[19] K.C. Kulander, J. Chem. Phys. 71 (1979) 2736–2737.
[20] T.R. Faulkner, J. Chem. Phys. 71 (1979) 2737.
[21] P.A. Malmqvist, N. Forsberg, Chem. Phys. 228 (1998) 227–240.
[22] A.M. Mebel, Y.-T. Chen, S.H. Lin, Chem. Phys. Lett. 258 (1996) 53–62.
[23] A.M. Mebel, M. Hayashi, K.K. Liang, S.H. Lin, J. Phys. Chem. A103 (1999) 10674–10690.
[24] K.K. Liang, H.J. Weber, M. Hayashi, S.H. Lin, in: Recent Research Developments in Physical Chemistry, vol. 8, Transworld Research Network, Kerala, India, 2005, p. 163.
[25] J.L. Chang, J. Mol. Spectrosc. 232 (2005) 102–104.
[26] C.L. Lee, S.H. Yang, S.Y. Kou, J.L. Chang, J. Mol. Spectrosc. 256 (2009) 279–286.
[27] J.L. Chang, J. Chem. Phys. 128 (2008). 174111/1–10.
[28] J. Liang, H. Zheng, X. Zhang, R. Li, Z. Cui, Mol. Phys. 105 (2007) 1903–1907.
[29] J. Liang, C.F. Liu, C.C. Wang, Z.C. Cui, Mol. Phys. 107 (2009) 2601–2608.
[30] J. Liang, R. Wang, X. Liang, C. Pan, F. Yang, Z. Cui, Mol. Phys. 109 (2011) 1727–1737.
[31] A. Twarowoki, Combust. Flame 102 (1995) 41–54.
[32] E.J.P. Zegers, E.M. Fisher, Combust. Flame 115 (1998) 230–240.
[33] O.P. Korobeinichev, S.B. Ilyin, V.M. Shvartsberg, A.A. Chernov, Combust. Flame 118 (1999) 718–726.
[34] M.A. MacDonald, T.M. Jayaweera, EI.M. Fisher, F.C. Gauldin, Combust. Flame 116 (1999) 166–176.
[35] O.P. Korobeinichev, S.B. Ilyin, T.A. Bolshova, V.M. Shvartsberg, A.A. Chernov, Combust. Flame 121 (2000) 593–609.
[36] K. Kawaguchi, S. Saito, E. Hirota, N. Ohashi, J. Chem. Phys. 82 (1985) 4893–4902.
[37] P.A. Hamilton, J. Chem. Phys. 86 (1987) 33–41;
H.-B. Qian, P.B. Davis, I.K. Ahmad, P.A. Hamilton, Chem. Phys. Lett. 235 (1995) 255–259.
[38] L. Andrews, R. Withnall, J. Am. Chem. Soc. 110 (1988) 5605–5611.

[39] R. Withnall, L. Andrews, J. Phys. Chem. 92 (1988) 4610–4619.
[40] C.W. Bauschlicher, M. Zhou, L. Andrews, J. Phys. Chem. A104 (2000) 3566–3571.
[41] M. McCluskey, L. Andrews, J. Phys. Chem. 95 (1991) 2988–2994.
[42] L.B. Knight Jr., G.C. Jones, G.M. King, R.M. Babb, A.J. McKinley, J. Chem. Phys. 103 (1995) 497–505.
[43] J. Lei, A. Teslja, B. Nizamov, P.J. Dagdigian, J. Phys. Chem. A 105 (2001) 7828–7833.
[44] L.L. Lohr, J. Phys. Chem. 88 (1984) 5569–5574.
[45] L.L. Lohr, R.C. Boehm, J. Phys. Chem. 91 (1987) 3203–3207.
[46] Y. Kabbadj, J. Lievin, Phys. Scripta 40 (1989) 259–269.
[47] S.A. Jarrett-Sprague, I.H. Hillier, I.R. Gould, Chem. Phys. 140 (1990) 27–33.
[48] Z.L. Cai, G. Hirsch, R.J. Buenker, Chem. Phys. Lett. 255 (1996) 350–356.
[49] J.S. Francisco, J. Chem. Phys. 117 (2002) 3190–3195.
[50] E.P.F. Lee, D.K.W. Mok, J.M. Dyke, F.T. Chau, J. Phys. Chem. A 106 (2002) 10130–10138.
[51] Z. Mielke, M. McCluskey, L. Andrews, Chem. Phys. Lett. 165 (1990) 146–154.
[52] S.J. Hunter, K.W. Hipps, A.H. Francis, Chem. Phys. 39 (1979) 209–220.
[53] C. Xu, E. de Beer, D.M. Neumark, J. Chem. Phys. 104 (1996) 2749–2751.
[54] X. Zhang, J. Wu, F. Wang, Z. Cui, J. Mol. Struct. (THEOCHEM) 851 (2008) 40–45.
[55] E.W. Weisstein, CRC Concise Encyclopedia of Mathematics, Chapman & Hall/CRC, Boca Raton, 2003.
[56] Gaussian 09, Revision A.02, written by M.J. Frisch, G.W. Trucks, H.B. Schlegel, G.E. Scuseria, M.A. Robb, J.R. Cheeseman, G. Scalmani, V. Barone, B. Mennucci, G.A. Petersson, H. Nakatsuji, M. Caricato, X. Li, H.P. Hratchian, A.F. Izmaylov, J. Bloino, G. Zheng, J.L. Sonnenberg, M. Hada, M. Ehara, K. Toyota, R. Fukuda, J. Hasegawa, M. Ishida, T. Nakajima, Y. Honda, O. Kitao, H. Nakai, T. Vreven, J.A. Montgomery, Jr., J.E. Peralta, F. Ogliaro, M. Bearpark, J.J. Heyd, E. Brothers, K.N. Kudin, V.N. Staroverov, R. Kobayashi, J. Normand, K. Raghavachari, A. Rendell, J.C. Burant, S.S. Iyengar, J. Tomasi, M. Cossi, N. Rega, J.M. Millam, M. Klene, J.E. Knox, J.B. Cross, V. Bakken, C. Adamo, J. Jaramillo, R. Gomperts, R.E. Stratmann, O. Yazyev, A.J. Austin, R. Cammi, C. Pomelli, J.W. Ochterski, R.L. Martin, K. Morokuma, V.G. Zakrzewski, G.A. Voth, P. Salvador, J.J. Dannenberg, S. Dapprich, A.D. Daniels, O. Farkas, J.B. Foresman, J.V. Ortiz, J. Cioslowski, and D.J. Fox, Gaussian, Inc., Wallingford CT, 2009.